TOWARD OPTIMAL VIDEO TRANSCODING

Ora Gendler and Moshe Porat

Department of Electrical Engineering, Technion - Israel Institute of Technology
Haifa 32000, Israel, phone: + 972-4-8294684, fax: +972-4-8295757
orag@tx.technion.ac.il, mp@ee.technion.ac.il

ABSTRACT

Real-time multimedia applications often require efficient bit-rate reduction. This is mainly done by requantization, usually in the DCT domain. This work introduces theoretical rate-distortion analysis that allows for straightforward selection of the quantization step needed to achieve a given bit-rate. The analysis is based on the Laplace-like distribution of DCT coefficients in the transform domain and on the structure of the quantizers commonly used in video and image coding. We show that the proposed transcoding design achieves significant compression at relatively low distortion, while keeping the computational complexity very low, allowing for real-time implementation.

1. INTRODUCTION AND PROBLEM DEFINITION

Visual communication often requires adjustment of the transmission bit-rate according to the bandwidth of the available channels, display characteristics and limitations of the end users. This raises the need for bit-rate reduction of the data stream, known as transcoding or transrating. For real-time applications, it is crucial that the transcoding will be of low computational complexity, while ensuring low distortion. A straightforward approach to transcoding is using quantization in various stages of image compression. It can be shown that the performance of requantization depends mainly on the ratio between the quantization step used for the initial quantization and the step used for requantization [1], [2]. So far, however, the performance of this straightforward transcoding approach has not been thoroughly analyzed for video sequences.

This work introduces theoretical analysis of requantization applied to still images and video in the DCT domain. The process of requantization consists of two stages. The first stage of quantization occurs at the source and thus cannot be controlled once done. The second stage of quantization is performed for transcoding and the quantizer can be freely designed. Accordingly, the focus of this work is on the analysis and design of the second stage quantizer for coded images and video, such as JPEG and MPEG. It is assumed that the first quantization takes place after a subband transform, such as DCT, has been applied to the image, block by block. The first stage quantizer, denoted by Q_1, performs uniform quantization using step size q_1. Alternatively, Q_1 could be applied using a quantization matrix, multiplied by the quality factor q_1. Though the analysis in this work refers to uniform quantization, the results apply to quantization using a quantization matrix as well, as shown in Section 3.

The second stage quantizer is denoted by Q_2 and the quantization step size (or quality factor) used is q_2. In addition to Q_1 and Q_2, a third reference quantizer is used, denoted by $Q_{2,\text{ref}}$. This coarse reference quantizer is used directly on the original coded image (not yet quantized) and also referred to as 'direct quantization'. The performance of the second stage quantizer is compared to that of the reference quantizer.

Throughout this work two types of quantizers are used: uniform threshold quantizer (UTQ) and UTQ-DZ (UTQ with dead zone), as in [1] and [3]. UTQ is used for still images and intra-frames of MPEG (I), while UTQ-DZ is used for inter frames. For UTQ, the quantizer definitions for the input $x \in R$ are:

$$\begin{aligned} &x_{Q1} = Q_1(x) = Round(x / q_1) \\ &Q_1^{-1}(x_{Q1}) = x_{Q1} \cdot q_1 \\ &Q_2(x_{Q1}) = Round\left(Q_1^{-1}(x_{Q1}) / q_2\right) \\ &Q_{2,ref}(x) = Round(x / q_2) \end{aligned} \tag{1}$$

The decision and reconstruction levels (for the positive axis) for the UTQ are defined as

$$d_{i,0} = 0;\quad d_{i,l} = (l - 0.5) q_i;\quad r_{i,0} = 0;\quad r_{i,l} = l \cdot q_i, \tag{2}$$

where the decision level l of the quantizer of Stage i (i=1,2) is denoted by $d_{i,l}$ and the reconstruction level is denoted by $r_{i,l}$. The definitions in (2) are symmetrical for the negative axis. For UTQ-DZ the definitions for the input $x \in R$ are given by:

$$\begin{aligned} &x_{Q1} = Q_1(x) = sign(x) \cdot Floor(abs(x) / q_1) \\ &Q_1^{-1}(x_{Q1}) = \left(x_{Q1} + 0.5 \cdot sign(x_{Q1})\right) \cdot q_1 \\ &Q_2(x_{Q1}) = sign(x_{Q1}) \cdot Floor\left(abs\left(Q_1^{-1}(x_{Q1})\right) / q_2\right) \\ &Q_{2,ref}(x) = sign(x) \cdot Floor(abs(x) / q_2). \end{aligned} \tag{3}$$

For this quantizer, the decision and reconstruction levels (for the positive axis) are defined as:

$$d_{i,0} = 0;\quad d_{i,l} = l q_i;\quad r_{i,0} = 0;\quad r_{i,l} = (l + 0.5) \cdot q_i. \tag{4}$$

As shown in [1], to avoid additional distortion resulting from performing the quantization in two stages rather than applying the coarse reference quantizer directly to the original image, the following condition should be met.

$$\forall x : Q_2(Q_1(x)) = Q_{2,ref}(x) \tag{5}$$

As shown in [1] [2] and [3], a necessary condition to achieve (5) is that the new requantization step be a multiple of the first stage quantization step size, so that

$$q_2 = k \cdot q_1,\ \ k \in \mathbb{N}\,. \tag{6}$$

The main goal of the present work is to analyze this condition and provide conclusions as to the preferred requantization step. Based on our analysis, an efficient real-time transcoding system can be easily designed, avoiding presently available complex approaches to transcoding.

This paper is organized as follows. Section 2 provides theoretical analysis of requantization and considers the main rounding policies. In Section 3 experimental results are presented, and in Section 4 the work is summarized and concluded.

2. RATE-DISTORTION ANALYSIS AND ROUNDING POLICY

Rate-distortion analysis is often performed to evaluate a transcoding system. Such analysis is instrumental in the design of a second stage quantizer and requires developing rate and distortion expressions for the requantized image. The rate can be expressed via the entropy, while the distortion can be expressed using an acceptable distortion criteria, such as MSE.

Our analysis requires modeling of the probability distribution of the DCT coefficients at the input and at the output of the first stage quantizer, as well as at the output of the second stage quantizer, marked as points A, B and C respectively, in Fig. 1.

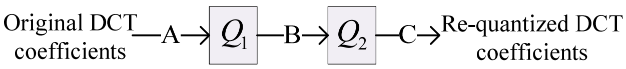

***Figure 1**: Quantization stages illustration*

We use the fact that the DCT coefficients at point A, before quantization, can be modeled using Laplace distribution [4]:

$$p(x) = 0.5\lambda e^{-\lambda|x|}\,. \tag{7}$$

At point B, after the first quantization, the DCT coefficients are discrete according to the representation levels of the first stage quantizer. The probability of each coefficient value is the total probability weight of the first stage quantization bin, represented by this value. For instance, level $r_{1,l}$ represents bin #l and has the probability weight $w_{1,l}$ obtained by integrating the Laplace distribution function over bin #l>0, as shown in the following equation

$$w_{1,l} = 0.5\lambda\int_{(l-0.5)q_1}^{(l+0.5)q_1} e^{-\lambda x}dx = 0.5e^{-\lambda(l-0.5)q_1}\left(1-e^{-\lambda q_1}\right) \tag{8}$$

for UTQ, and in:

$$w_{1,l} = 0.5\lambda\int_{lq_1}^{(l+1)q_1} e^{-\lambda x}dx = 0.5e^{-\lambda(l+1)q_1}\left(e^{\lambda q_1}-1\right) \tag{9}$$

for UTQ-DZ, for $x \geq 0$, while for $x < 0$ the expressions are symmetrical.

Accordingly, the distribution of the discrete values at point C has to be modeled. As a result of requantization, several quantization bins of the first stage quantizer are represented by one second-stage representation level. This happens since each second-stage quantization bin contains an integer number of first stage quantization bins (required to maintain (5), as shown in [5]) and thus the probability weight of this second stage representation level is the sum of probability weights of the first stage quantization bins inside. This is illustrated in Fig. 2, for the case of $q_2 = 4{\cdot}q_1$, where

$$w_{2,l} = w_{1,4l} + w_{1,4l+1} + w_{1,4l+2} + w_{1,4l+3};\ \ l > 0\,. \tag{10}$$

The merging of probability weights and thus the resulting requantization performance depends mainly on the position of second stage decision levels relative to the first stage decision levels. However, it is also affected by the rounding method of the second-stage quantizer, which is addressed in the next subsection.

2.1 Rounding Policy Effects

When performing division during requantization with the quantizer defined in (1) and (2), it is possible to round the value of 0.5 to 0 or 1. Let us consider an example where $q_1 = 3$ and $q_2 = 2{\cdot}q_1 = 6$. At the second-stage quantizer there are two options to quantize the value 3 (a representation level of the first stage quantizer) since it falls exactly on the decision level of the second-stage quantizer. This value could be quantized to either 0 or 6, according to the chosen rounding policy: $Q_2(3) = Round^{RTZ}(3/6) = 0$, namely 'Rounding Toward Zero' (*RTZ*), or $Q_2(3) = Round^{RR}(3/6) = 1$, regarded as 'Regular Rounding' (*RR*). Similarly, -3 could be quantized to 0 or -1.

When using UTQ and q_2 is selected as an even multiple of q_1, this ambiguity occurs for every other quantization bin. Thus, the rounding policy of the second stage quantizer can significantly affect the results. When using UTQ-DZ, the rounding policy will have no effect, since no first step representation level could ever collide with second step representation level, when (6) applies. If we assume that this collision ($r_{1,l} = d_{2,m}$) does happen for some l and m, then we obtain the following condition:

$$(l+0.5)q_1 = mq_2 = mkq_1 \Rightarrow (l-mk)q_1 = 0.5q_1\,. \tag{11}$$

Since m,l and k are integers, the above could never hold.

2.2 Bit-rate and Distortion Analysis

The bit-rate after requantization is analyzed here as a function of k (as defined in (6)) for both rounding methods and quantizer types. Only integer values are considered since an integer ratio is required to avoid added distortion due to the requantization process and since it allows for detailed analysis regardless of the first stage quantization step q_1. Generally, for UTQ and odd values of k, the rate and distortion of both rounding methods are identical. This is concluded by using distortion expressions developed for both rounding methods in [6] and the entropy expression in Table 1. The reason is that when k is odd, the decision levels of the second-stage quantizer do not cause rounding ambiguity. The bit-rate is analyzed using the entropy obtained by:

$$H = -\sum_{l=-\infty}^{\infty} p\left(r_{2,l}\right)\log_2 p\left(r_{2,l}\right), \tag{12}$$

where $r_{2,l}$ is, as before, the representation level of quantization bin #l of the second quantizer. For UTQ, the entropy expressions are derived separately for odd and even values of k. UTQ expressions for entropy are shown in Table 1 and an example of the results for both rounding methods and direct quantization is plotted in Fig. 3.. Here $q_1 = 10$ and the Laplace parameter was $\lambda = 0.1$, an appropriate value for typical images [4]. It can be observed that for *RTZ*, a much steeper decrease in entropy occurs when k is even. This shows that better compression can be achieved at these points. As for *RR*, a steeper decrease in entropy occurs when k is odd. In general, the entropy is substantially lower for *RTZ*, showing that this method achieves better compression. When comparing to the direct quantization curve, i.e., applying the coarse reference quantizer directly to the original data, it can be observed that for the even values of k, the entropy of direct quantization is larger than when *RTZ* is used and smaller than the entropy obtained when *RR* is used. At the odd values, however, all three methods perform equally. UTQ-DZ entropy expression (valid for all integer k's and both rounding methods) is shown in Table 2.

Similarly, expressions for distortion as a function of k were developed using (13), for both rounding methods. The expressions for UTQ-DZ are presented in Table 3. The UTQ expressions were developed in [6].

$$D = \int_{-\infty}^{\infty} \left(x - \hat{x}\right)^2 f\left(x\right) dx = \frac{1}{2} \lambda \sum_{l=-\infty}^{\infty} \int_{d_{2,l}}^{d_{2,l+1}} \left(x - r_{2,l}\right)^2 e^{-\lambda|x|} dx \quad (13)$$

The expressions for rate and distortion are used to create theoretic rate-distortion graphs, which appear in Fig. 4 (left) for UTQ-DZ and Fig. 5 (left) for UTQ. For UTQ-DZ the behavior of the graph is the same for requantization using both rounding methods and for direct quantization. For UTQ the behavior is more interesting and is further analyzed. The numerical values used to create the graph in Fig. 5 appear in Table 4. It can be seen that: (i) *RTZ* usually outperforms *RR* and direct quantization, i.e., it provides lower distortion for the same rate. (ii) For both rounding methods, there are areas where lowering the rate slightly results in a substantial increase in distortion. Interestingly, when using *RR*, there is a point where substantially reducing the rate (from 2.26 to 1.69 bits/pixel) decreases the distortion as well (from 58 to 54). This is due to the way the probability weights of the first stage representation levels merged during requantization. (iii) The points of intersection for all three methods are the odd multiples of the original step size, i.e., odd values of k. (iv) Generally, *RR* achieves the worst results.

3. EXPERIMENTAL RESULTS

The right parts of Fig. 4 and Fig. 5 show the empirical averaged rate-distortion for UTQ-DZ and UTQ, respectively. For UTQ-DZ inter frames were used, while for UTQ still images were used. It can be seen that for both quantizers, the behavior observed is very similar to that shown in the theoretical rate-distortion graphs in the left parts of Fig. 4 and Fig. 5.

The values of rate and distortion differ in the two parts of Fig. 4 and Fig. 5 since one side is theoretical and the other is experimental. For UTQ, as mentioned earlier, *RTZ* provides better results. In addition, there are several requantization steps that perform poorly, increasing the distortion substantially for a minor rate decrease. The numerical results are summarized in Table 4. For UTQ-DZ, the behavior is rather smooth.

Fig. 6 shows results for requantization using a typical quantization matrix and UTQ. A frame from ‘Foreman’ sequence is shown in Fig. 6 (top) and was first quantized using the quality factor $q_1 = 0.5$ and then requantized using the requantization quality factor $q_2 = 1$. Fig. 6 (middle) shows the requantized frame, using *RR*. Fig. 6 (bottom) shows the requantized frame, using *RTZ*. It can be observed that the bottom image (*RTZ*) is much smoother and less noisy, has a higher PSNR (by almost 2 dB) and significantly lower bitrate. These results are consistent with the theoretical analysis and show the major role of the rounding method in the design of the second stage quantizer. Furthermore, this shows that the analysis carried out for uniform quantization can be applied to quantization using a quantization matrix. This can be readily explained by the uniform quantization applied to each DCT coefficient with the appropriate quantization step from the matrix.

Fig. 7 shows the PSNR Vs. frame number, for 'Foreman' and 'Bus' in CIF resolution with 'IPPPP' GOP, initially quantized with $q_1 = 0.5$, and then requantized with $q_2 = 1$, for direct quantization and both rounding methods. *RTZ* outperforms *RR* and is close to direct quantization performance (slightly lower PSNR at a slightly lower rate).

4. CONCLUSIONS

We have derived a rate-distortion curve of requantized images and video frames as a function of the ratio between the first and the second quantization steps. These expressions provide a useful rate-distortion function for image and video recompression and transcoding. This analysis allows for a straightforward design of the second stage quantizer used for bit-rate reduction. Our analysis shows that in order to achieve the best compression ratio, one has to requantize the DCT coefficients of images and intra frames using an even multiple of the original quantization step. To keep the distortion low at these points, rounding toward zero should be applied. When requantizing the inter frames, any integer multiple of the original quantization step can be used. In all cases, the selection of the specific multiple should be made based on the rate-distortion expressions, obtained with an appropriate value of the Laplace parameter λ for each frequency band. The requantization step could be then determined based on the required bit-rate and acceptable distortion. Our new approach can be also applied to other data types with the appropriate distribution [7]. Our conclusion is that this analysis is instrumental in designing transcoding systems, allowing for real-time implementation due to its very low complexity.

	H[bits per pixel] as a function of $k=q_2/q_1$
RR, k even	$\lambda\int_0^{0.5(k-1)q_1} e^{-\lambda x}dx\cdot\log_2\left(0.5\lambda\int_0^{0.5(k-1)q_1} e^{-\lambda x}dx\right)+\sum_{l=1}^{\infty}\left[\lambda\int_{(kl-0.5(k+1))q_1}^{(kl+0.5(k-1))q_1} e^{-\lambda x}dx\cdot\log_2\left(0.5\lambda\int_{(kl-0.5(k+1))q_1}^{(kl+0.5(k-1))q_1} e^{-\lambda x}dx\right)\right]=$ $=\frac{e^{-0.5(k-1)\lambda q_1}}{\ln(4)}\left\{\begin{matrix}-(2k-1)\lambda q_1-k\lambda q_1\coth[0.5k\lambda q_1]+\\ 2\left(e^{0.5(k-1)\lambda q_1}-1\right)\cdot\ln\left(0.5-0.5e^{-0.5(k-1)\lambda q_1}\right)+2\ln\left(0.5-0.5e^{k\lambda q_1}\right)\end{matrix}\right\}$
RTZ, k even	$\lambda\int_0^{0.5(k+1)q_1} e^{-\lambda x}dx\cdot\log_2\left(0.5\lambda\int_0^{0.5(k+1)q_1} e^{-\lambda x}dx\right)+\sum_{l=1}^{\infty}\left[\lambda\int_{(kl-0.5(k-1))q_1}^{(kl+0.5(k+1))q_1} e^{-\lambda x}dx\cdot\log_2\left(0.5\lambda\int_{(kl-0.5(k-1))q_1}^{(kl+0.5(k+1))q_1} e^{-\lambda x}dx\right)\right]=$ $=\left(2\ln\left[0.5-0.5e^{-0.5(k+1)\lambda q_1}\right]-e^{-0.5(k+1)\lambda q_1}\left((2k+1)\lambda q_1+k\lambda q_1\coth[0.5k\lambda q_1]+2\ln\left[\frac{1-e^{-0.5(k+1)\lambda q_1}}{e^{k\lambda q_1}-1}\right]\right)\right)\Big/\ln(4)$
RR & RTZ, k odd	$\lambda\int_0^{0.5kq_1} e^{-\lambda x}dx\cdot\log_2\left(0.5\lambda\int_0^{0.5kq_1} e^{-\lambda x}dx\right)+\sum_{l=1}^{\infty}\left[\lambda\int_{k(l-0.5)q_1}^{k(l+0.5)q_1} e^{-\lambda x}dx\cdot\log_2\left(0.5\lambda\int_{k(l-0.5)q_1}^{k(l+0.5)q_1} e^{-\lambda x}dx\right)\right]=\log_2(e)\left(e^{1.5k\lambda q_1}-e^{0.5k\lambda q_1}\right)\cdot$ $\cdot\left(-k\lambda q_1e^{k\lambda q_1}+e^{1.5k\lambda q_1}\ln\left[0.5-0.5e^{-0.5k\lambda q_1}\right]+\left(e^{k\lambda q_1}-1\right)\ln\left[1+e^{0.5k\lambda q_1}\right]+e^{0.5k\lambda q_1}\ln\left[1+\coth(0.25k\lambda q_1)\right]\right)$

Table 1: *UTQ Entropy analysis of requantized data for two rounding methods (RTZ and RR)*

	H[bits per pixel] as a function of $k=q_2/q_1$
RR & RTZ, k even or odd	$\lambda\int_0^{kq_1} e^{-\lambda x}dx\cdot\log_2\left(\lambda\int_0^{kq_1} e^{-\lambda x}dx\right)+\sum_{l=1}^{\infty}\left[\lambda\int_{klq_1}^{(kl+k)q_1} e^{-\lambda x}dx\cdot\log_2\left(0.5\lambda\int_{klq_1}^{(kl+k)q_1} e^{-\lambda x}dx\right)\right]=$ $=\log_2(e)\left[k\lambda q_1\left(e^{-k\lambda q_1}-2\right)\Big/\left(e^{k\lambda q_1}-1\right)-e^{-k\lambda q_1}\ln\left(2\Big/\left(e^{k\lambda q_1}-1\right)\right)+\left(1-e^{-k\lambda q_1}\right)\ln\left(1-e^{-k\lambda q_1}\right)\right]$

Table 2: *UTQ-DZ Entropy analysis of requantized data*

	MSE as a function of $k=q_2/q_1$
RR & RTZ, k even or odd	$\lambda\int_0^{kq_1} x^2e^{-\lambda x}dx+\sum_{l=1}^{\infty}\left[\lambda\int_{klq_1}^{(l+1)kq_1}\left(x-\left(l+\frac{1}{2}\right)kq_1\right)^2e^{-\lambda x}dx\right]=\frac{2}{\lambda^2}+\frac{2kq_1}{\lambda\left(1-e^{k\lambda q_1}\right)}-e^{-k\lambda q_1}\left(\frac{kq_1}{\lambda}+\frac{3k^2q_1^2}{4}\right)$

Table 3: *UTQ-DZ Distortion analysis of requantized data*

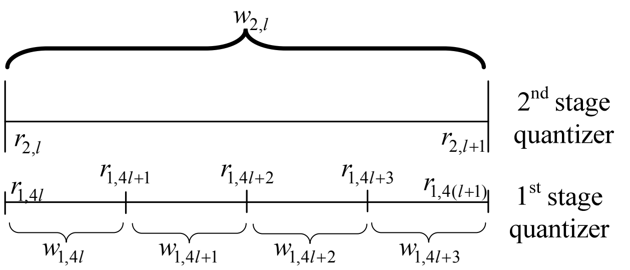

Figure 2: *Illustration of one 2nd stage quantization bin containing four 1st stage quantization bins.*

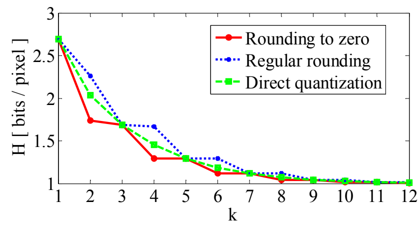

Figure 3: *UTQ Theoretical entropy of requantized Laplace distribution originally quantized with $q_1 = 10$, as a function of $k= q_2/ q_1$ for both rounding methods and direct quantization.*

5. REFERENCES

[1] A. Leventer and M. Porat, "Towards optimal bit-rate control in video transcoding", IEEE International Conference on Image Processing, ICIP 2003, Vol. 3, pp.265-8, 2003.

[2] H.H Bauschke, C.H.Hamilton, M.S Macklem, J.S McMichael, and N.R Swart, "Recompression of JPEG images by requantization" ,IEEE Trans. Image Processing, Vol. 12, pp. 843 - 849, 2003.

[3] O. Werner, "Requantization for transcoding of MPEG-2 Intra frames," IEEE Trans. on Image Proc., Vol. 8, pp.179-191, 1999.

[4] S. R. Smoot, L. A. Rowe, and E.F. Roberts, "Laplacian model for AC DCT terms in image and video coding," Proc. of the 13th International Workshop on Network and Operating Systems Support for Digital Audio and Video, Monterey, pp.60-9, 2003.

[5] O. Gendler and M.Porat, "On transcoding optimization using requantization" CCIT Report No. 717, Technion, Jan. 2009.

[6] O. Gendler and M. Porat, "On Efficient Quantization for Image Recompression", Eusipco 2009.

[7] M. Porat and Y.Y. Zeevi, "The generalized Gabor scheme of image representation in biological and machine vision", IEEE Trans. on Pattern Analysis and Machine Intelligence (PAMI) 10:44, pp. 452-468, 1988.

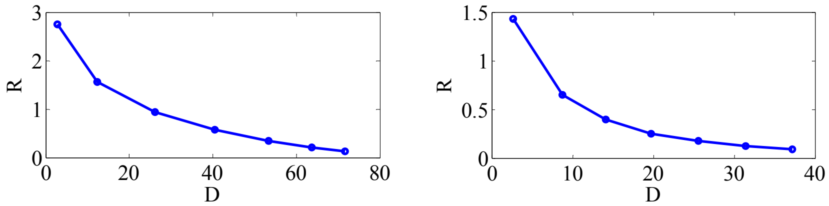

Figure 4: *UTQ-DZ rate vs. distortion for requantized Laplace data and inter frames, for q_1=4, where three re-quantization methods coincide. Left: Theoretical rate-distortion for Laplace data with λ=0.15. Right: Experimental results obtained by averaging 16 inter frames. As can be seen, the graphs demonstrate similar behavior.*

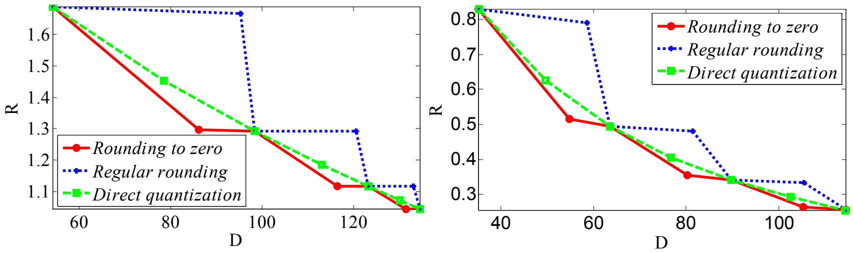

Figure 5: *UTQ rate vs. distortion for q_1=10, using both rounding methods. Direct quantization is also shown. Left: Theoretical rate-distortion for requantized Laplace data with λ=0.1. Right: Experimental rate vs. distortion, averaged for 7 images. As can be seen, the graphs demonstrate similar behavior, with rounding-to-zero outperforming regular rounding.*

$k=\frac{q_2}{q_1}$	R-D function				Simulation			
	D		*R [bpp]*		*D*		*R [bpp]*	
	RTZ	*RR*	*RTZ*	*RR*	*RTZ*	*RR*	*RTZ*	*RR*
1	8	8	2.7	2.7	7	7	1.96	1.96
2	42	**58**	1.74	2.26	29	**43**	0.90	1.67
3	54	**54**	1.69	1.69	35	**35**	0.83	0.83
4	86	95	1.30	1.67	55	59	0.52	0.79
5	98	98	1.29	1.293	66	64	0.49	0.49
6	116	120	1.1163	1.292	80	81	0.35	0.48
7	123	123	1.1162	1.1162	90	90	0.34	0.34

Table 4: *Rate vs. distortion as a function of k. Theoretical results (left) were calculated for q_1=10. Simulation results (right) are the average for 7 images, initially quantized with q_1=10. Note that RR performs very poorly at even values of k (in theory and simulation) such that k=3 outperforms k=2 (**bold**).*

Figure 6: *A frame from 'Foreman' for q_1=0.5 and q_2=1 using a quantization matrix. Top: Original. Middle: Regular rounding, with PSNR=32.63dB at 1.35 bit/pixel. Bottom: Rounding toward zero, with PSNR=34.59dB, at 0.83 bit/pixel. As can be seen, Rounding toward zero outperforms Regular rounding.*

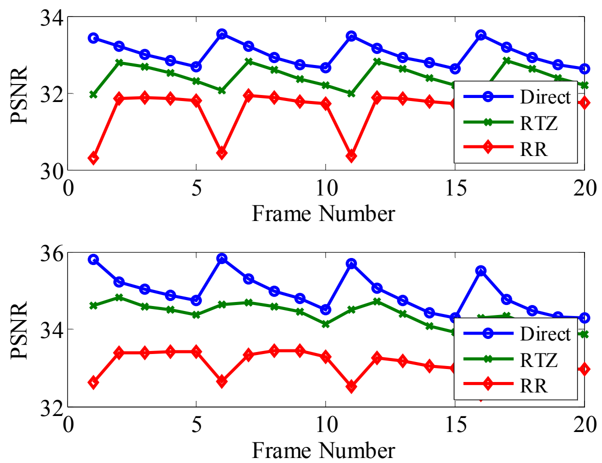

Figure 7 (Left): *PSNR vs. frame number for 'Bus' (top) and 'Foreman'(bottom) at q_1=0.5 and q_2=2·q_1=1 using a quantization matrix, for direct quantization and for both rounding methods. RTZ (avg. rate of 1.04 and 0.39 bit/pixel) outperforms RR (avg. rate 1.26 and 0.57 bit/pixel), and is close to direct quantization (at 1.09 and 0.43 bit/pixel), for 'Bus' and' Forman', respectively.*